REPORT DOCUMENTATION PAGE

Form Approved
OMB No. 0704-0188

1. REPORT DATE *(DD-MM-YYYY)*	**2. REPORT TYPE**	**3. DATES COVERED** *(From - To)*
May 2012	Technical Paper	May 2012-July 2012

4. TITLE AND SUBTITLE
Low Noise Fractional NTC Collisions for DSMC

5a. CONTRACT NUMBER
In-House

5b. GRANT NUMBER

5c. PROGRAM ELEMENT NUMBER

6. AUTHOR(S)

Robert Scott Martin and Jean-Luc Cambier

5d. PROJECT NUMBER

5e. TASK NUMBER

5f. WORK UNIT NUMBER
23041057

7. PERFORMING ORGANIZATION NAME(S) AND ADDRESS(ES)

Air Force Research Laboratory (AFMC)
AFRL/RQRS
1 Ara Drive.
Edwards AFB CA 93524-7013

8. PERFORMING ORGANIZATION REPORT NO.

9. SPONSORING / MONITORING AGENCY NAME(S) AND ADDRESS(ES)
Air Force Research Laboratory (AFMC)
AFRL/RQR
5 Pollux Drive
Edwards AFB CA 93524-7048

10. SPONSOR/MONITOR'S ACRONYM(S)

11. SPONSOR/MONITOR'S REPORT NUMBER(S)
AFRL-RZ-ED-TP-2012-210

12. DISTRIBUTION / AVAILABILITY STATEMENT
Distribution A: Approved for Public Release; Distribution Unlimited. PA#12552

13. SUPPLEMENTARY NOTES
Conference paper for the 28th International Symposium on Rarefied Gas Dynamics, Zaragoza, Spain, 9-13 July 2012.

14. ABSTRACT
The ability to accurately simulate rare high energy collisions such as those found in ionization and combustion reactions is important to the advancement of the study of non-equilibrium behavior of these phenomena. A major difficulty for modeling these systems with particle codes is that chain-branching reactions result in exponential growth regimes for certain species. This work considers the use of fractional collision models in place of statistically sampled collision models combined with merging of computational particles to reduce statistical noise while avoiding runaway computational cost.

15. SUBJECT TERMS

16. SECURITY CLASSIFICATION OF:			**17. LIMITATION OF ABSTRACT**	**18. NUMBER OF PAGES**	**19a. NAME OF RESPONSIBLE PERSON**
					Jean-Luc Cambier
a. REPORT	**b. ABSTRACT**	**c. THIS PAGE**			**19b. TELEPHONE NO** *(include area code)*
Unclassified	**Unclassified**	**Unclassified**	SAR	55	661-275-5649

Low Noise Fractional NTC Collisions for DSMC

Robert Scott Martin* and Jean-Luc Cambier†

*ERC Inc.,
†Spacecraft Propulsion Branch,
Air Force Research Laboratory,
Edwards AFB, CA 93524 USA

Abstract. The ability to accurately simulate rare high energy collisions such as those found in ionization and combustion reactions is important to the advancement of the study of non-equilibrium behavior of these phenomena. A major difficulty for modeling these systems with particle codes is that chain-branching reactions result in exponential growth regimes for certain species. This work considers the use of fractional collision models in place of statistically sampled collision models combined with merging of computational particles to reduce statistical noise while avoiding runaway computational cost.

Keywords: Particle Merge, Particle in Cell, PIC, Adaptive Methods
PACS: 51.xxxx

INTRODUCTION

The advent of the 'no-time-counter' (NTC) collisional sampling technique by Bird[1] greatly contributed to the proliferation of DSMC codes used throughout the rarefied gas dynamics field by making physically relevant gas dynamics problems computationally accessible. This was achieved by sampling only a fraction of possible collision pairs and adjusting the probability of collision to account for the skipped collisions. The technique produces physically accurate collision rates for gases and gas mixtures in both equilibrium and non-equilibrium[2] flows. However for some types of rare collisions such as inelastic ionization processes, this approach results in significant noise.

For any particle technique, resolving the tails of the velocity distribution function (VDF) is necessarily difficult. By definition, the tail represents a large volume of velocity space yet only a small fraction of the total number of particles. Many of the special inelastic collisions found in plasma and combustion processes require overcoming an energy barrier. They therefore disproportionately rely on collisions by particles in this tail.

When only a few computational particles can be devoted to resolving the tails, what should be represented as a large number of low probability events is instead represented by a single infrequent event involving a large fraction of the probability in that region of the VDF. Suppressing this noise requires large numbers of particles so that more than just a few particles resolve the relevant tail of the VDF.

An example of this behavior can be seen in Bird's 0D study of ignition delay time using the quantum-kinetic chemistry model[3]. The delay time appears to converge only when using greater than between 10e5-10e6 particles. This is a result of the relatively low probability of chain initiation reactions. Such a high particle count quickly becomes intractable for any higher dimensionality flow.

FRACTIONAL COLLISIONS

Consider a modification of the NTC collisional sampling approach to allow for collision of only a fraction of the number of real particles represented by each computational particle, i.e. a fraction of the statistical 'weight'. For every collision pair selected, the collision partner weights are then reduced by a fraction that depends on the collision probability instead of performing an 'all or nothing' collision for the pair depending on whether a random number exceeds a probability threshold, the defining characteristic of 'Monte Carlo' methods. The fraction of real particles

participating in the collision is then applied to newly created particles such that the result of the collision conserves the total weight.

Although more conceptually straightforward than the sampling only a subset of possible collisions and randomly selecting whether they occur as in the original NTC method, this approach rapidly increases the number of computational particles in the simulation. The approach therefore requires an efficient conservative particle merging technique that maintains important non-equilibrium features of the velocity distribution. In this work, the authors' approach for particle merging described in the companion paper, Reference [4], is used to counteract this growth in computational particles.

With this approach, the number of collisions to perform out of the possible N(N-1)/2 combinations becomes another tunable parameter for the simulation. The few particles that occupy the tails of the velocity distribution have a disproportionately high impact on the higher order moments of the the distribution just as outliers in a statistical distribution impact the RMS value more than the mean. For the simulations presented, the number of collisions selected was set by the formula shown in Equation 1. For this

$$N_{collision} = fN_p log(N_p) \tag{1}$$

As the number of fractional collisions sampled is increased, the magnitude of the change of moments becomes smaller for any given timestep. Rare collisions involving the distribution tail that would otherwise only occur every few timesteps if at all instead scatter a small fraction of the probability in the tails every timestep. Even though the average number of particles scattered out of the tail is equal across many timesteps, it is hoped that the fractional collisions offer a possibility for smoother and more tightly coupled collisional evolution.

BI-MAXWELLIAN THERMALIZATION RESULTS

To examine the performance of this new collision sampling technique, consider the thermalization of a bi-Maxwellian distribution with equal y- and z-temperatures, but a bimodal x-temperature. For the cases presented, the thermal components of the distributions were initialized to 300K in y- and z-directions and 150K in the x-direction. The centers of the halves of the bimodal distribution were set to $\pm$750 m/s and the gas used was Argon. Collisions were based on a VSS collision cross section with parameters from the appendix of Reference [1].

Figure 1 shows that the rate of thermal relaxation for 10 separate cases using the identical initial particle distributions for the original NTC method and the new fraction collision algorithm. The original NTC method uses 800 particles for this test case. For the fractional algorithm, the fraction parameter $f = 10^{-1/2}$ was used for the example shown. The merge algorithm's target number of particles was 800, but the actual average number of post merge macro particles was only 587. This number was the result of a balance with the fraction parameter and merge aggressiveness parameters. The fractional collisions resulted in an average peak of 2914 particles prior to merging back down to 587.

Figure 2 shows these same 10 cases where the mean temperatures and RMS of the deviation from the mean for each timestep were calculated. The lines and error bars from the plots are these means and $\pm$RMS values respectively. Though the mean temperatures are quite consistent, the variance of the temperature components in time match those of a NTC run with many more computational particles.

To quantify the correlation between RMS temperature error and the number of particles at various stages of the fraction collision and merge process, a matrix of original and fractional collision runs were performed. The original collision model was run with 50, 100, 200, 400, and 800 initial particles. The fractional collision model was run using the original 800 particles from the 800 particle original case, but with target particle numbers of 50, 100, 200, 400, and 800. This array of target particle numbers was also run at three different collision fraction parameters, f, of 10^{-1}, $10^{-1/2}$, 10^{0}. The RMS temperature error was then collected for each of these cases as well as the pre- and post-collision number of macro particles.

Figure 3 shows the effect of varying the number of particles on the RMS error. The variance in temperature of the new method appears to be controlled nearly independently from the pre-collision number of particles. Instead it depends on the peak number of particles resulting from fractional collisions prior to merging. Because the number of collision partners to select out of the possible N(N-1)/2 pairs is an independent parameter, the temperature variance can be controlled directly at the expense of more aggressive particle merging at the end of the collision step as quantified by the f parameter.

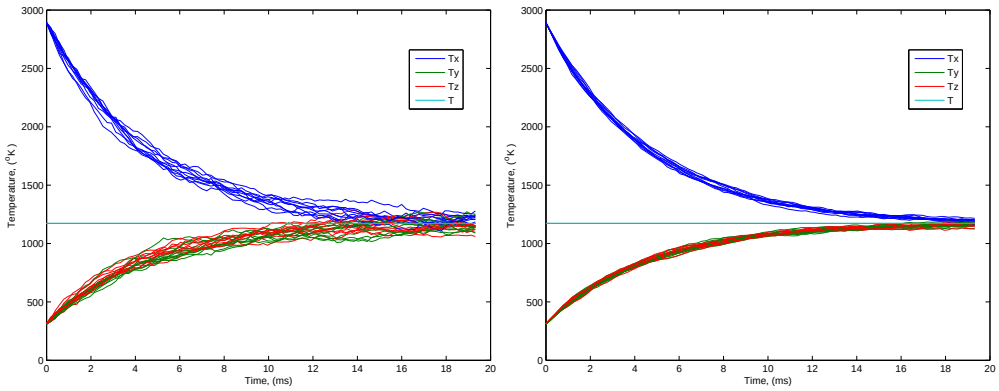

FIGURE 1. Thermal relaxation of anisotropic temperature for initially bi-Maxwellian temperature distribution. Plot shows 10 separate cases from the same initial particle velocity distribution. Results for the original NTC collisions are shown on the left and fractional NTC collisions are on the right.

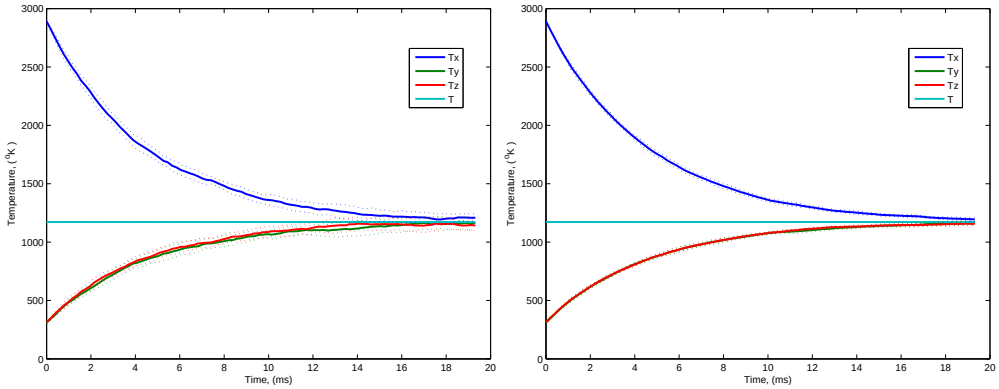

FIGURE 2. Thermal relaxation of anisotropic temperature for initially bi-Maxwellian temperature distribution. Plot shows mean and RMS error-bars of 10 separate cases from the same initial particle velocity distribution. Results for the original NTC collisions are shown on the left and fractional NTC collisions are on the right.

COLLISIONAL BEAMS IN POTENTIAL WELL

Having shown that at least thermalization rate in the 0D sense matches between the original and fractional-NTC collision algorithms, it is important to determine whether these the fractional collision and accompanying merge can reproduce the evolution of particles that are also moving between cells spatially. To test the fractional collision in 1D rather than 0D, a charged particle version of the bi-Maxwellian is placed within a 1-D electrostatic potential well such that the two oscillating beams interact when they cross at the bottom of the well. Though the particles are charged in the sense that an external force accelerates them towards the spatial center, only the elastic particle collisions are considered and modeled with a VSS collision cross section. Consideration of effective-Coulomb collisions is considered later.

Figure 4 shows that the variable soft sphere (VSS) thermalization of the oscillating beams matches well between the two collision sampling techniques. The figure also shows that both the NTC and new fractional-NTC can produce similar number density evolution despite dramatically different numbers of computational particles per cell.

Unfortunately, the authors know of no exact solution for this crossed beam thermalization problem. Higher fidelity simulations using traditionally accepted particle methods are left to future work to determine whether the fractional collision provides any advantage over traditional methods.

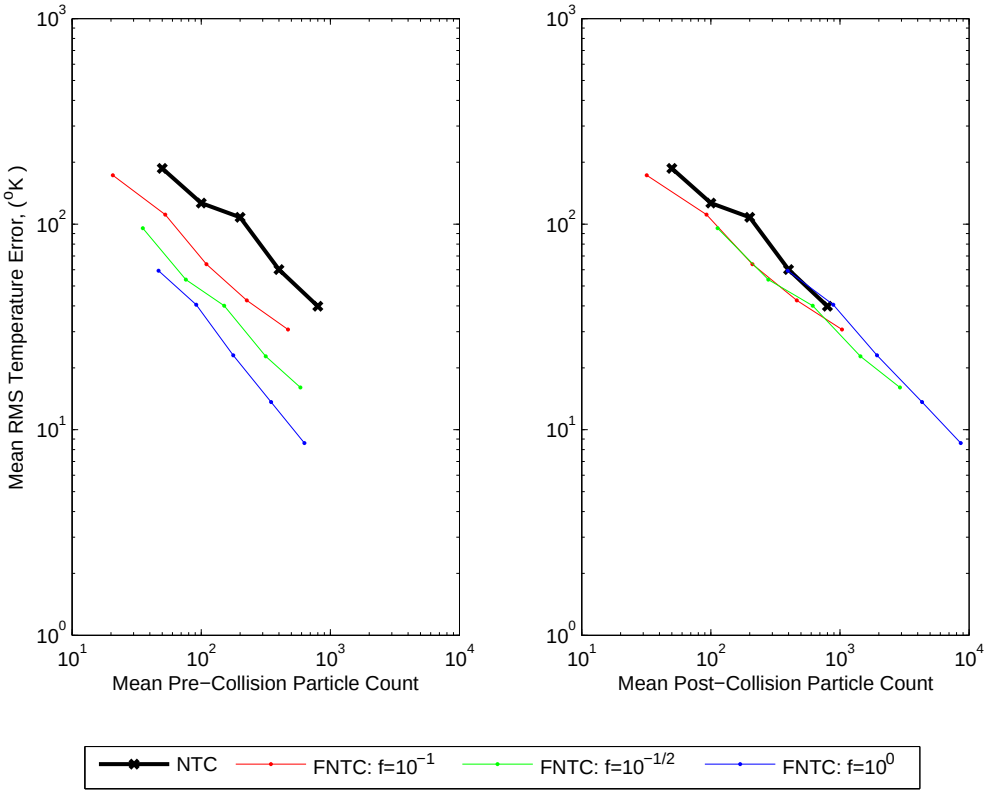

FIGURE 3. Temperature RMS error relative to the mean temperature on average for all timesteps relative to the number of macro particles. The left plot shows the pre-collision average number of macro-particles as the x-coordinate while the right plot shows the same error levels with the post-collision average number of macro-particles. The line colors depict the fractional-NTC aggressiveness parameter.

FRACTIONAL MCC IONIZATION EVENTS

For a second test of fractional collisions with merging, a electron avalanche in a spark gap gas breakdown is considered as it was in the companion paper, Reference [4]. The simulation is initialized with a 6kV potential drop across a 5mm gap. The evolution of electron density is studied in a partially ionized background Argon gas which is assumed stationary for the duration of the simulation.

The inelastic MCC collision model previously used for the electron avalanche is modified to remove the random nature in place of a fractional collision as it was with the NTC elastic collisions. The number of collisions per timestep is calculated exactly as it was in Reference [4]. Instead of selecting collisions that exceed a probability ratio based on that collision frequency, the number of colliding particles is removed from the original particle weight and two new particles are created following the formula shown in Equation 2.

$$\mathrm{Ar}^0 + e^- \rightarrow (1-\alpha)\left(\mathrm{Ar}^0 + e^-_{original}\right) + \alpha\left(\mathrm{Ar}^+ + e^-_{scattered} + e^-_{emitted}\right) \tag{2}$$

One of the new particles represents the fraction of initial particles involved in the collision. The velocity of this particle is reduced by the ionization energy necessary for the collision. This new computational particles weight is simply the number of collisions per timestep used to reduce the original particle's weight.

The second of the new particles represent the electron ejected from the background neutral gas. This particle again has a numerical weight equal to the number of collisions per timestep, but its velocity is zero.

Though this collision algorithm triples the number of computational particles in every timestep, the merging algorithm effectively maintains the target number of computational particles preventing runaway growth. Figure 5 compares the results for the original MCC, merged MCC, and merged fractional-MCC algorithms for the spark gap.

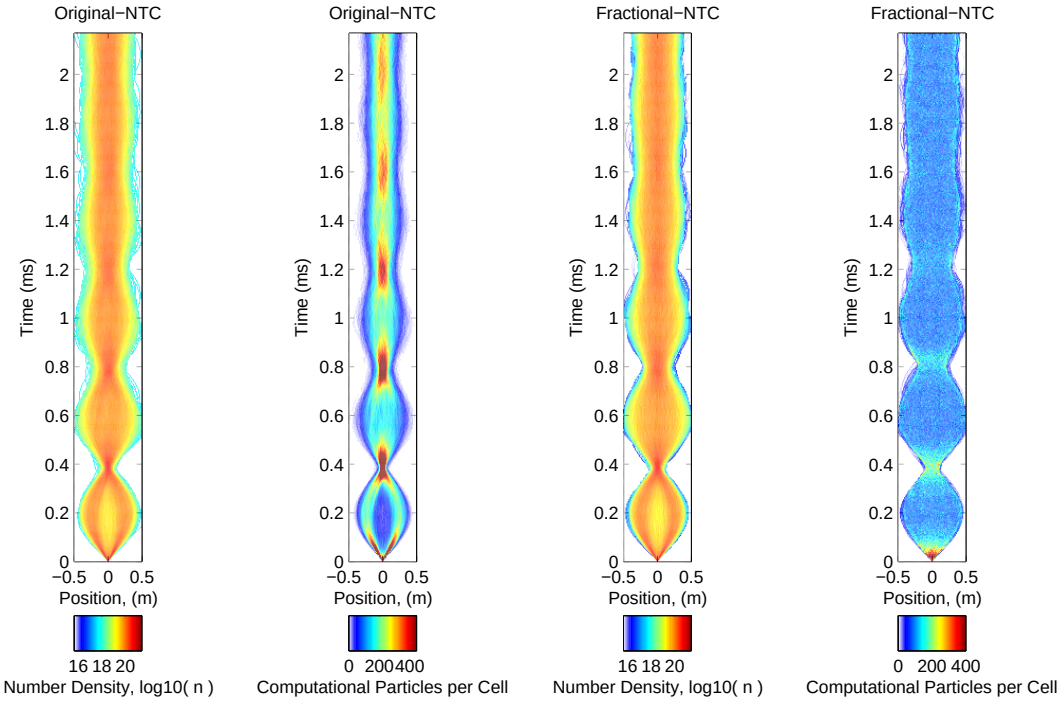

FIGURE 4. Position vs Time results of number density and computational particles per cell in thermalizing oscillating beams. The left figures are for the original NTC method with fixed particle weight. The right figures are for the the fractional-NTC collisions along with octree merge algorithms.

Two key differences between the fractional and original MCC algorithms are apparent. First, the fractional MCC algorithm has less 'streaks' because the ionization occurs more frequently with smaller magnitude. The most apparent streak is the vertical yellow stripe crossing the original rarefaction edge at approximately 4mm and 0.2ns in the merged MCC example. The other key difference is that the fractional-MCC results become noisier in general above approximately 0.3ns. This is likely the result of a considerably more aggressive merge. With the fractional-MCC algorithm, every electron above the threshold energy results in the production of 2 slower particles with potentially tiny weights due to extremely small cross sections and low probability. This large quantity of nearly weightless particles may be overwhelming the octree-merge. A higher fidelity reference case is needed to further quantify 'correctness' in the absence of an exact analytical solution for the ionizing spark.

Though the electron density evolution looks similar between the MCC and fractional-MCC collision methods, one area in which the fractional-MCC method particularly excelled was in the smoothness of the positive ion profile. Because the fractional MCC collision event creates particles with only a fraction of the weight of the original, the ion density is incremented in a smooth fashion between cells and timesteps. However, again because no analytical or very high fidelity solution exists, it is impossible to determine if these results are 'better' or not with the current tools. Again, higher fidelity baseline simulations are needed to determine whether the fractional collision model is actually more predictive.

FUTURE EXTENSION AND CONCLUDING REMARKS

In addition to studying fractional elastic and inelastic ionizing collisions, a model for an effective Coulomb collision is also currently under consideration. Without such a model, the populations of free streaming and post-collision or post-ejection electrons have no mechanism to thermalize.

Unfortunately, the cross section for Coulomb collisions diverges without a cutoff to the integral at the Debye radius. This cutoff is ill-defined in a highly non-equilibrium sense. Short of modeling the full N-body interaction, or at least the multi-pole expansion thereof, a simplified collision model is needed.

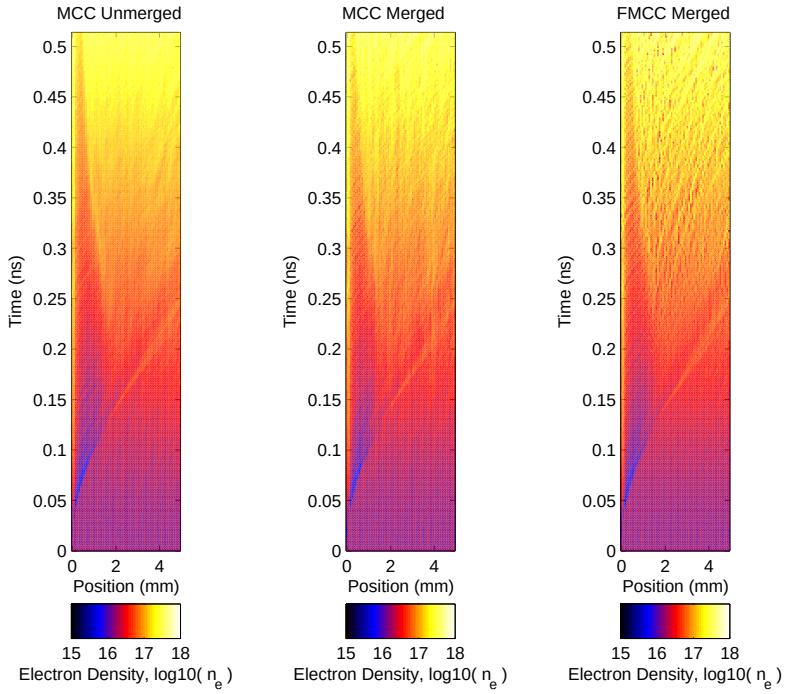

FIGURE 5. Position vs Time diagram of electron density and computational particles per cell in an ionizing spark gap using MCC collision model. Electrons are pushed from the cathode on the left to anode on the right of the figures due to the 6kV applied potential. The left figure shows the original MCC collision model with fixed particle weight and the middle figure shows the original MCC collision model for the octree merge algorithm. The right figure shows the fractional-MCC model with octree merge.

Such a simplified approximate model based on Zel'dovich's approach to estimating electron conductivity [5] is considered. Equation 3 shows this effective cross section for Coulomb collisions from Zel'dovich, though the leading constant is given without justification. The model estimates an effective cross section and collision frequency for which the accumulation of many small angle Coulomb collisions results in a momentum change of the order of the original velocity. The Coulomb logarithm, $ln\Lambda$, accounts for the cutoff to bound the collision integral for 'far' interactions.

$$\sigma = 0.69\pi \frac{Z^4 e^4{}^2}{kT}\ ln\Lambda \tag{3}$$

The same basic approach was used by Kapper and Cambier [6] to estimate the electron-ion thermalization in their two-fluid Argon shock ionization collisional radiative studies. As these results compared well to Schlieren and interferogram experimental results, applying this effective approximate Coulomb collision appears to be a good starting point for electron thermalization and conductivity in PIC codes. The expectation would be that the electron conductivity would the at least be consistent between particle and fluid models near equilibrium and would provide initial insight into the potential breakdown when moving away from equilibrium.

For an initial study of self-thermalization of electrons, the cross section of Equation 3 was modified by replacing the temperature with relative velocity as $kT = \frac{1}{2}mv_r^2$. Though only approximately correct, the goal was to at least achieve the correct near-equilibrium thermalization rate when the temperatures are well defined.

Several 0D electron thermalization cases were performed, but relaxation rates appeared to be highly dependant on time step and merge parameters. Though further investigation is needed,

it is thought that this result may be due to the $\propto T^{-2}$ dependence of the cross section on temperature in conjunction to the particle merge. The hard sphere model has a temperature dependence related to $T^{1/2}$ and the VHS and VSS models vary between $T^{1/2}$ and T^1. The poor performance of the pseudo-Coulomb collision might be a result of the merge only conserving moments through $\overline{v^2}$ while the Coulomb cross section depends on $\overline{v^4}$. The high order velocity dependence means that the effective Coulomb relaxation is highly dependent on the shape of the tail of the distribution

that is not necessarily preserved by the merge. Hopefully this effect can be mitigated in the future with a merge that conserves higher moments as initially outlined in the companion merge paper[4].

REFERENCES

1. G. Bird, *Molecular Gas Dynamics and the Direct Simulation of Gas Flows*, Oxford University Press, 1994.
2. G. Bird, "Perception of numerical methods in rarefied gas dynamics," in *Proc. 16th Int. Symp. on Rarefied Gas Dynamics*, American Institute of Aeronautics and Astronautics, Pasadena, California, 1988, pp. 221–226.
3. G. Bird, *Physics of Fluids* **23**, 106101 (2011).
4. R. Martin, and J.-L. Cambier, "Moment Preserving Adaptive Particle Weights using Octree Velocity Distributions for PIC Simulations," 2012.
5. Y. B. Zel'dovich, and Y. Raizer, *Physics of Shock Waves and High-Temperature Hydrodynamic Phenomena*, Dover, 2002.
6. M. Kapper, and J.-L. Cambier, *J. Appl. Phys.* **109**, 113309 (2011).

Low Noise Fractional NTC Collisions for DSMC

Robert Martin & Jean-Luc Cambier

ERC Inc.,
Spacecraft Propulsion Branch
Air Force Research Laboratory
Edwards Air Force Base, CA USA

U.S. AIR FORCE

28th International Symposium on Rarefied Gas Dynamics

Outline

Importance of Collision Physics

Important Collisions in Spacecraft Propulsion:

- Discharge and Breakdown in FRC
- Collisional Radiative Cooling/Ionization
- Combustion Chemistry

Common Features in Spacecraft Collisions:

- Relevant Densities Spanning Many Orders of Magnitude — 6+
- Transitions from Collisional to Collisionless
- Tiny Early e^- or Radical Populations Critical to Induction Delay
- Many types of Inelastic Collisions with Unknown Effects on Distribution Shapes

Shock Ionization

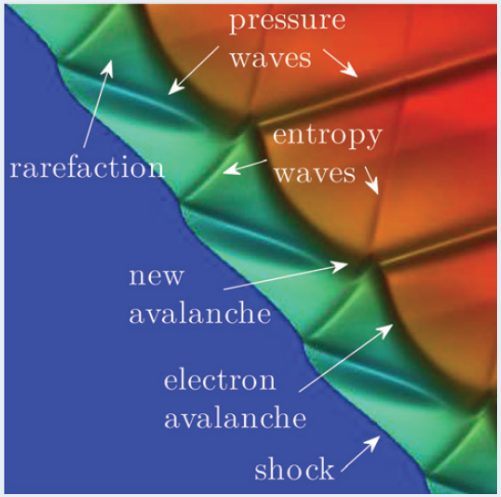

Kapper & Cambier, J. Appl. Phys. 109, (2011)

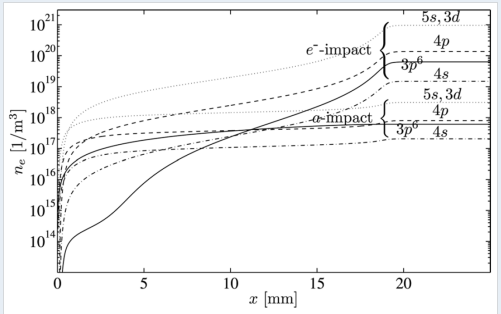

Importance of Collision Physics

Important Collisions in Spacecraft Propulsion:

- Discharge and Breakdown in FRC
- Collisional Radiative Cooling/Ionization
- Combustion Chemistry

Common Features in Spacecraft Collisions:

- Relevant Densities Spanning Many Orders of Magnitude — 6+
- Transitions from Collisional to Collisionless
- Tiny Early e^- or Radical Populations Critical to Induction Delay
- Many types of Inelastic Collisions with Unknown Effects on Distribution Shapes

Need Low Noise & High Dynamic Range Collision Algorithms

Shock Ionization

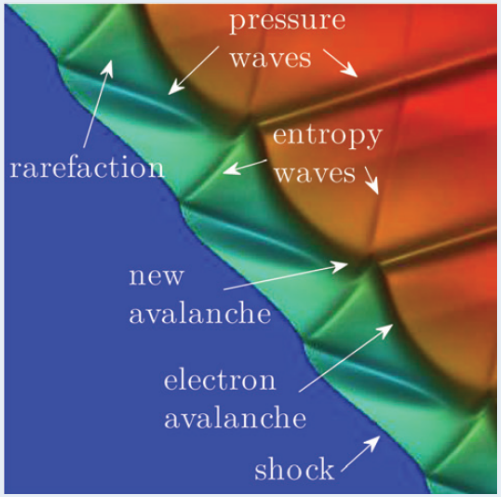

Kapper & Cambier, J. Appl. Phys. 109, (2011)

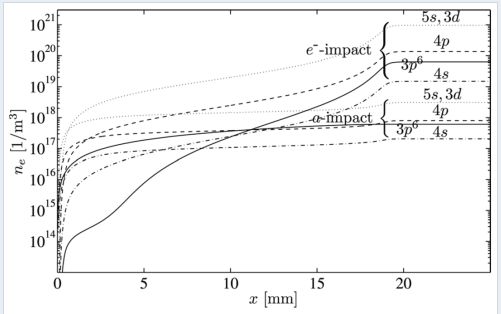

Previous Collision Methods:

- Monte Carlo Collisions (MCC)
  - Particles Collide with Background "Fluid"
  - Often Used in Plasma/PIC Simulation
  - Ion-e^- Collisions Assume Stationary Ions
  - No Conservation/Detailed Balance
- Direct Simulation Monte Carlo Collisions (DSMC)
  - Most Modern Versions use No-Time Counter (NTC) Method
  - Conservative/Reversible Collision
  - Satisfies Detailed Balance
  - Subset of Possible Collisions Sampled
  - Random Selection vs Z_{ij} for All/Nothing Collision

All Random Flip vs Number of Collisions: $Z_{ij} = \frac{n_i n_j}{2} \langle \sigma v \rangle \, \mathrm{dt}$

Inelastic NTC Issues

Continuum to Discrete Representation:

- Many Particles $\rightarrow$ Effectively Continuous Distribution

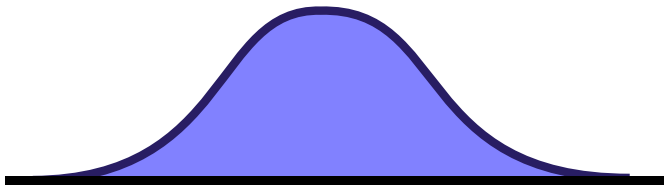

Inelastic NTC Issues

Continuum to Discrete Representation:

- Many Particles $\rightarrow$ Effectively Continuous Distribution
- Discretized VDF yields Fokker-Planck
  But Collision Integral Still a Problem

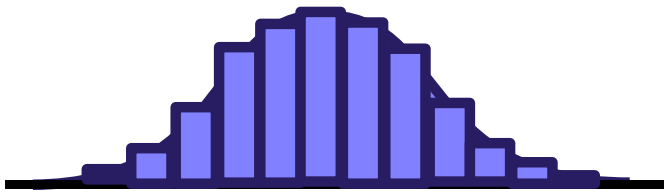

Inelastic NTC Issues

Continuum to Discrete Representation:

- Many Particles $\rightarrow$ Effectively Continuous Distribution
- Discretized VDF yields Fokker-Planck
  But Collision Integral Still a Problem
- Particle Methods Simplify to Delta Functions
- Collisions between Discrete Velocities

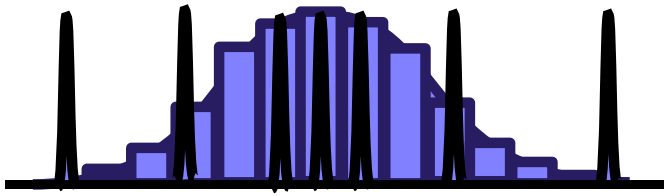

Inelastic NTC Issues

Continuum to Discrete Representation:

- Many Particles $\rightarrow$ Effectively Continuous Distribution
- Discretized VDF yields Fokker-Planck But Collision Integral Still a Problem
- Particle Methods Simplify to Delta Functions
- Collisions between Discrete Velocities
- Inelastic Collisions Particularly Impact High Order Moments

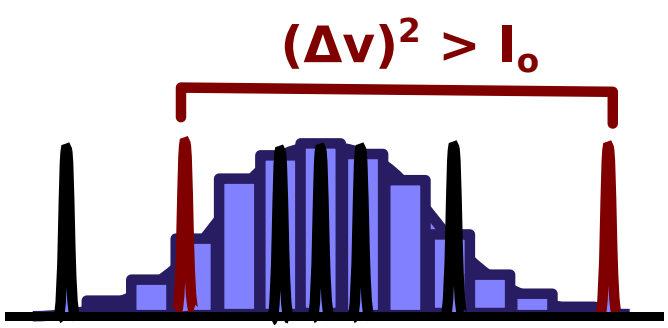

Inelastic NTC Issues

Continuum to Discrete Representation:

- Many Particles $\rightarrow$ Effectively Continuous Distribution
- Discretized VDF yields Fokker-Planck But Collision Integral Still a Problem
- Particle Methods Simplify to Delta Functions
- Collisions between Discrete Velocities
- Inelastic Collisions Particularly Impact High Order Moments
- All-or-Nothing Collision Yields Rare Large Magnitude Changes

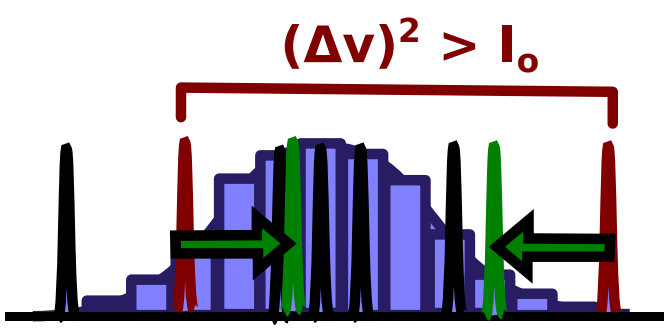

Fractional Collision Concept

Partial Collisions:

- Variable Particle Weights allow more DOF representing Tails

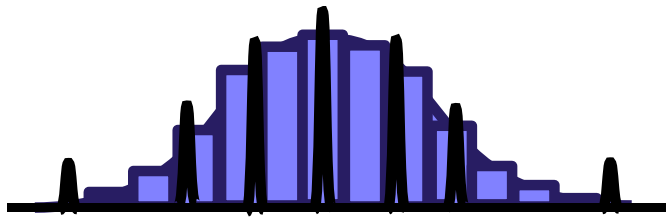

Fractional Collision Concept

Partial Collisions:

- Variable Particle Weights allow more DOF representing Tails
- Fraction of Particles for All Sampled Collisions Scattered Instead of Random "All-or-Nothing"

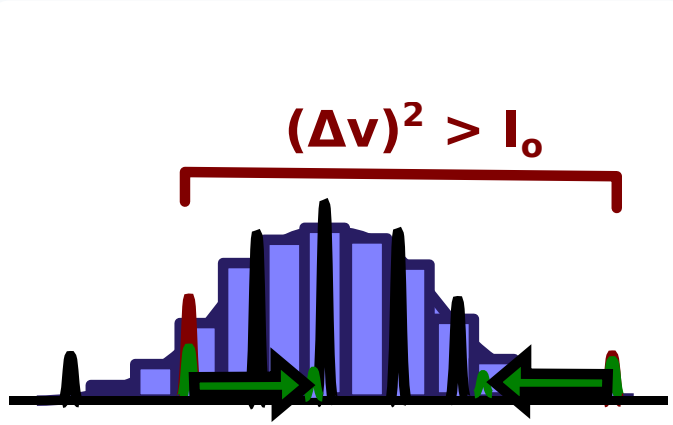

Fractional Collision Concept

Partial Collisions:

- Variable Particle Weights allow more DOF representing Tails
- Fraction of Particles for All Sampled Collisions Scattered Instead of Random "All-or-Nothing"
- Continuously Creates Numerical Particles

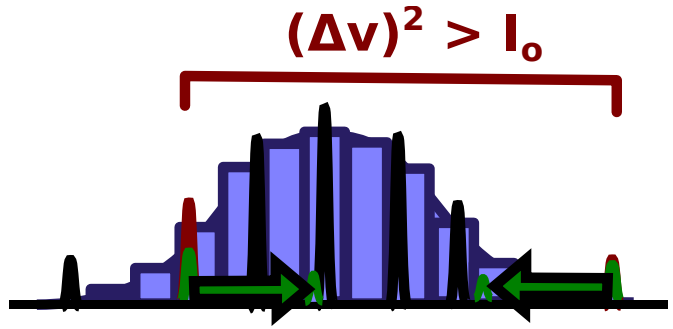

Fractional Collision Concept

Partial Collisions:

- Variable Particle Weights allow more DOF representing Tails
- Fraction of Particles for All Sampled Collisions Scattered Instead of Random "All-or-Nothing"
- Continuously Creates Numerical Particles
- Requires Conservative Particle Merge

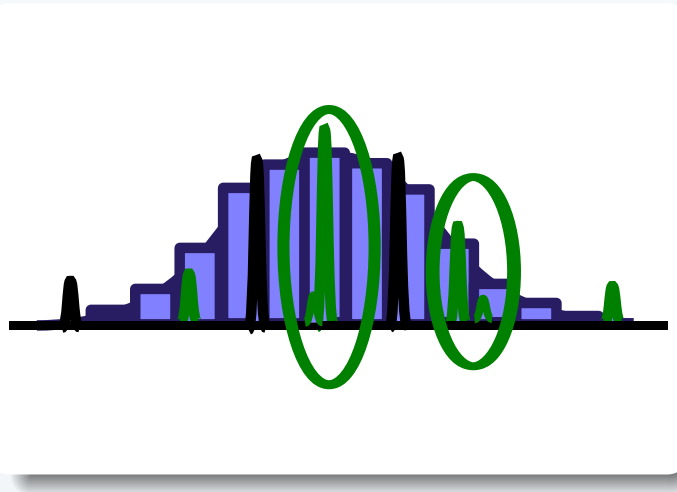

Fractional Collision Concept

Partial Collisions:

- Variable Particle Weights allow more DOF representing Tails
- Fraction of Particles for All Sampled Collisions Scattered Instead of Random "All-or-Nothing"
- Continuously Creates Numerical Particles
- Requires Conservative Particle Merge
- Merged Distribution Not Changed as Dramatically

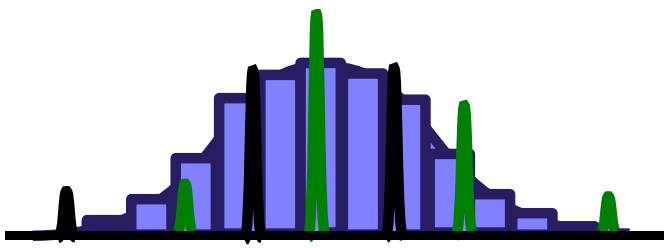

Fractional Collision Concept

Partial Collisions:

- Variable Particle Weights allow more DOF representing Tails
- Fraction of Particles for All Sampled Collisions Scattered Instead of Random "All-or-Nothing"
- Continuously Creates Numerical Particles
- Requires Conservative Particle Merge
- Merged Distribution Not Changed as Dramatically

Smoother Evolution of High Moments

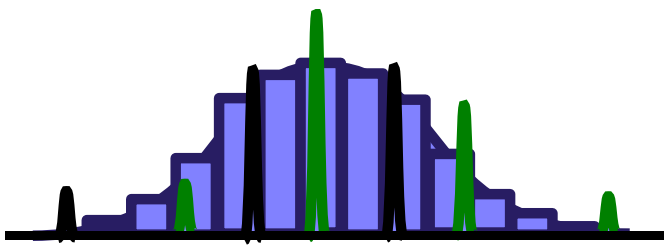

Fractional Collisions

NTC Collisions:

- Collision Rate Cell to Collision Volume Ratio

$$Z_{ij} = \frac{n_i n_j}{2} \langle \sigma v \rangle_{ij} \, \mathrm{dt} = \frac{w_i w_j}{2V_{cell}^2} \langle \sigma v \rangle_{ij} \, \mathrm{dt}$$

Fractional-NTC Collisions:

Fractional Collisions

NTC Collisions:

- Collision Rate Cell to Collision Volume Ratio
- Fraction of $N^2/2$ Possible Collisions Sampled

$$Z_{ij} = \frac{n_i n_j}{2} \langle \sigma v \rangle_{ij} \, \mathrm{dt} = \frac{w_i w_j}{2 V_{cell}^2} \langle \sigma v \rangle_{ij} \, \mathrm{dt}$$

$$P_{ij} = w \langle \sigma v \rangle_{ij} \, \mathrm{dt} / V_{cell}$$
$$P_{max} = w \langle \sigma v \rangle_{ij,max} \, \mathrm{dt} / V_{cell}$$
$$N_{select} = \frac{N_p^2}{2} F_n \langle \sigma v \rangle_{ij,max} \, \mathrm{dt} / V_{cell}$$

Fractional-NTC Collisions:

Fractional Collisions

NTC Collisions:

- Collision Rate Cell to Collision Volume Ratio
- Fraction of $N^2/2$ Possible Collisions Sampled
- Probability of Event Ratio of Volumes

$$Z_{ij} = \frac{n_i n_j}{2} \langle \sigma v \rangle_{ij} \, \mathrm{dt} = \frac{w_i w_j}{2 V_{cell}^2} \langle \sigma v \rangle_{ij} \, \mathrm{dt}$$

$$P_{ij} = w \langle \sigma v \rangle_{ij} \, \mathrm{dt} / V_{cell}$$
$$P_{max} = w \langle \sigma v \rangle_{ij,max} \, \mathrm{dt} / V_{cell}$$
$$N_{select} = \frac{N_p^2}{2} F_n \langle \sigma v \rangle_{ij,max} \, \mathrm{dt} / V_{cell}$$

Collide if:

$$\text{Rand}(1) < \frac{N_{collide}}{N_{select}} = \frac{P_{ij}}{P_{max}} = \frac{\langle \sigma v \rangle_{ij}}{\langle \sigma v \rangle_{ij,max}}$$

Fractional-NTC Collisions:

Fractional Collisions

NTC Collisions:

- Collision Rate Cell to Collision Volume Ratio
- Fraction of $N^2/2$ Possible Collisions Sampled
- Probability of Event Ratio of Volumes
- Yields Correct Non-Equilibrium Frequency

Fractional-NTC Collisions:

$$Z_{ij} = \frac{n_i n_j}{2} \langle \sigma v \rangle_{ij} \, \mathrm{dt} = \frac{w_i w_j}{2 V_{cell}^2} \langle \sigma v \rangle_{ij} \, \mathrm{dt}$$

$$P_{ij} = w \langle \sigma v \rangle_{ij} \, \mathrm{dt} / V_{cell}$$
$$P_{max} = w \langle \sigma v \rangle_{ij,max} \, \mathrm{dt} / V_{cell}$$
$$N_{select} = \frac{N_p^2}{2} F_n \langle \sigma v \rangle_{ij,max} \, \mathrm{dt} / V_{cell}$$

Collide if:

$$\mathrm{Rand}(1) < \frac{N_{collide}}{N_{select}} = \frac{P_{ij}}{P_{max}} = \frac{\langle \sigma v \rangle_{ij}}{\langle \sigma v \rangle_{ij,max}}$$

Fractional Collisions

NTC Collisions:

- Collision Rate Cell to Collision Volume Ratio
- Fraction of $N^2/2$ Possible Collisions Sampled
- Probability of Event Ratio of Volumes
- Yields Correct Non-Equilibrium Frequency

Fractional-NTC Collisions:

- Number of Collisions Selected by Computational Cost/Accuracy Tradeoff

$$Z_{ij} = \frac{n_i n_j}{2} \langle \sigma v \rangle_{ij} \, \mathrm{dt} = \frac{w_i w_j}{2 V_{cell}^2} \langle \sigma v \rangle_{ij} \, \mathrm{dt}$$

$$P_{ij} = w \langle \sigma v \rangle_{ij} \, \mathrm{dt} / V_{cell}$$
$$P_{max} = w \langle \sigma v \rangle_{ij,max} \, \mathrm{dt} / V_{cell}$$
$$N_{select} = \frac{N_p^2}{2} F_n \langle \sigma v \rangle_{ij,max} \, \mathrm{dt} / V_{cell}$$

Collide if:

$$\text{Rand}(1) < \frac{N_{collide}}{N_{select}} = \frac{P_{ij}}{P_{max}} = \frac{\langle \sigma v \rangle_{ij}}{\langle \sigma v \rangle_{ij,max}}$$

$$N_{select} = f \, N_p log(N_p)$$

Fractional Collisions

NTC Collisions:

- Collision Rate Cell to Collision Volume Ratio
- Fraction of $N^2/2$ Possible Collisions Sampled
- Probability of Event Ratio of Volumes
- Yields Correct Non-Equilibrium Frequency

Fractional-NTC Collisions:

- Number of Collisions Selected by Computational Cost/Accuracy Tradeoff
- Collision Δw Scaled for Skipped Collisions

$$Z_{ij} = \frac{n_i n_j}{2} \langle \sigma v \rangle_{ij} \, \mathrm{dt} = \frac{w_i w_j}{2 V_{cell}^2} \langle \sigma v \rangle_{ij} \, \mathrm{dt}$$

$$P_{ij} = w \langle \sigma v \rangle_{ij} \, \mathrm{dt} / V_{cell}$$
$$P_{max} = w \langle \sigma v \rangle_{ij,max} \, \mathrm{dt} / V_{cell}$$
$$N_{select} = \frac{N_p^2}{2} F_n \langle \sigma v \rangle_{ij,max} \, \mathrm{dt} / V_{cell}$$

Collide if:

$$\mathrm{Rand}(1) < \frac{N_{collide}}{N_{select}} = \frac{P_{ij}}{P_{max}} = \frac{\langle \sigma v \rangle_{ij}}{\langle \sigma v \rangle_{ij,max}}$$

$$N_{select} = f \, N_p log(N_p)$$

$$\Delta w_{ij,collide} = \frac{N_p^2/2}{N_{select}} Z_{ij}$$

Fractional Collisions

NTC Collisions:

- Collision Rate Cell to Collision Volume Ratio
- Fraction of $N^2/2$ Possible Collisions Sampled
- Probability of Event Ratio of Volumes
- Yields Correct Non-Equilibrium Frequency

$$Z_{ij} = \frac{n_i n_j}{2} \langle \sigma v \rangle_{ij} \, \mathrm{dt} = \frac{w_i w_j}{2 V_{cell}^2} \langle \sigma v \rangle_{ij} \, \mathrm{dt}$$

$$P_{ij} = w \langle \sigma v \rangle_{ij} \, \mathrm{dt} / V_{cell}$$
$$P_{max} = w \langle \sigma v \rangle_{ij,max} \, \mathrm{dt} / V_{cell}$$
$$N_{select} = \frac{N_p^2}{2} F_n \langle \sigma v \rangle_{ij,max} \, \mathrm{dt} / V_{cell}$$

Collide if:

$$\mathrm{Rand}(1) < \frac{N_{collide}}{N_{select}} = \frac{P_{ij}}{P_{max}} = \frac{\langle \sigma v \rangle_{ij}}{\langle \sigma v \rangle_{ij,max}}$$

Fractional-NTC Collisions:

- Number of Collisions Selected by Computational Cost/Accuracy Tradeoff
- Collision Δw Scaled for Skipped Collisions
- Particles Created & Original Weight Reduced

$$N_{select} = f \, N_p log(N_p)$$

$$\Delta w_{ij,collide} = \frac{N_p^2/2}{N_{select}} Z_{ij}$$

$$w_i = w_i - \Delta w_{ij} \;\&\; w_j = w_j - \Delta w_{ij}$$
$$w_{(N_p+1)} = \Delta w_{ij} \;\&\; w_{(N_p+2)} = \Delta w_{ij}$$

Fractional Collisions

NTC Collisions:

- Collision Rate Cell to Collision Volume Ratio
- Fraction of $N^2/2$ Possible Collisions Sampled
- Probability of Event Ratio of Volumes
- Yields Correct Non-Equilibrium Frequency

$$Z_{ij} = \frac{n_i n_j}{2} \langle \sigma v \rangle_{ij} \, \mathrm{dt} = \frac{w_i w_j}{2 V_{cell}^2} \langle \sigma v \rangle_{ij} \, \mathrm{dt}$$

$$P_{ij} = w \langle \sigma v \rangle_{ij} \, \mathrm{dt} / V_{cell}$$
$$P_{max} = w \langle \sigma v \rangle_{ij,max} \, \mathrm{dt} / V_{cell}$$
$$N_{select} = \frac{N_p^2}{2} F_n \langle \sigma v \rangle_{ij,max} \, \mathrm{dt} / V_{cell}$$

Collide if:

$$\mathrm{Rand}(1) < \frac{N_{collide}}{N_{select}} = \frac{P_{ij}}{P_{max}} = \frac{\langle \sigma v \rangle_{ij}}{\langle \sigma v \rangle_{ij,max}}$$

Fractional-NTC Collisions:

- Number of Collisions Selected by Computational Cost/Accuracy Tradeoff
- Collision Δw Scaled for Skipped Collisions
- Particles Created & Original Weight Reduced
- Note: If $\Delta w > w \rightarrow N_{select}$ is Increased

$$N_{select} = f \, N_p log(N_p)$$

$$\Delta w_{ij,collide} = \frac{N_p^2/2}{N_{select}} Z_{ij}$$

$$w_i = w_i - \Delta w_{ij} \;\&\; w_j = w_j - \Delta w_{ij}$$
$$w_{(N_p+1)} = \Delta w_{ij} \;\&\; w_{(N_p+2)} = \Delta w_{ij}$$

Bi-Maxwellian Thermalization Results

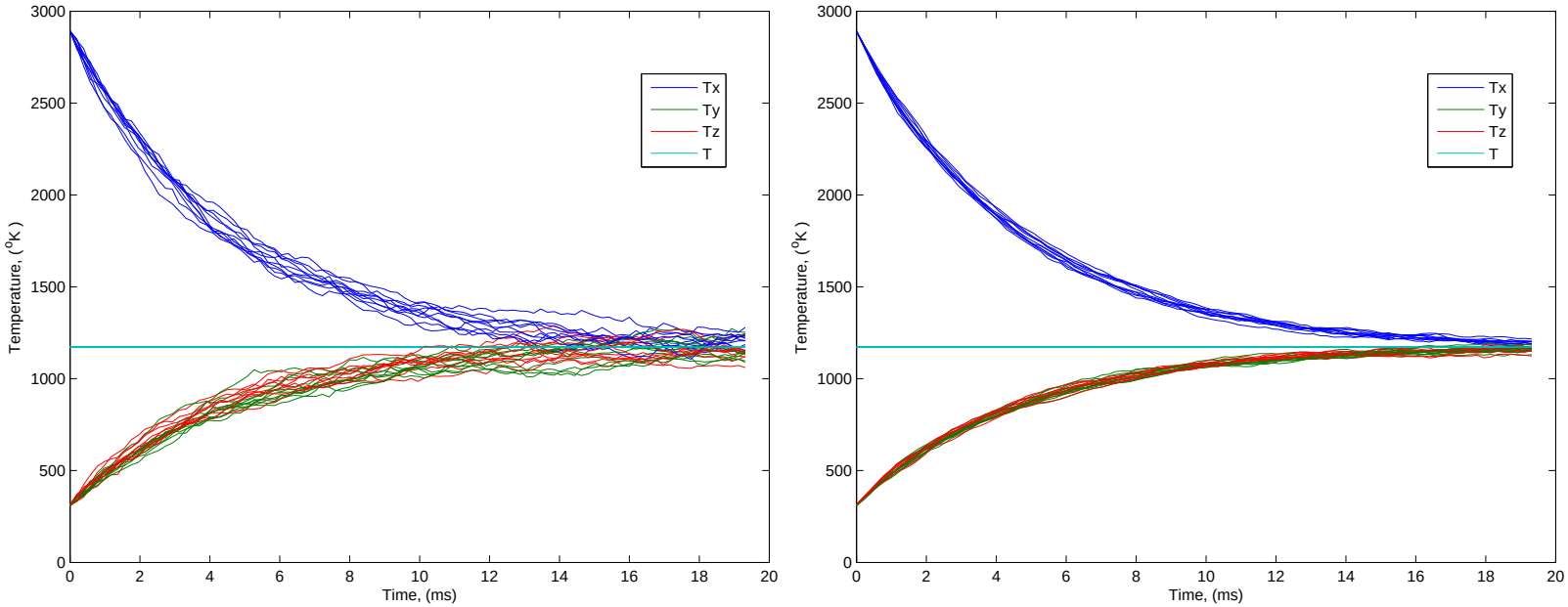

Comparison of 10x Runs from Same Initial Distribution

Bi-Maxwellian Thermalization Results

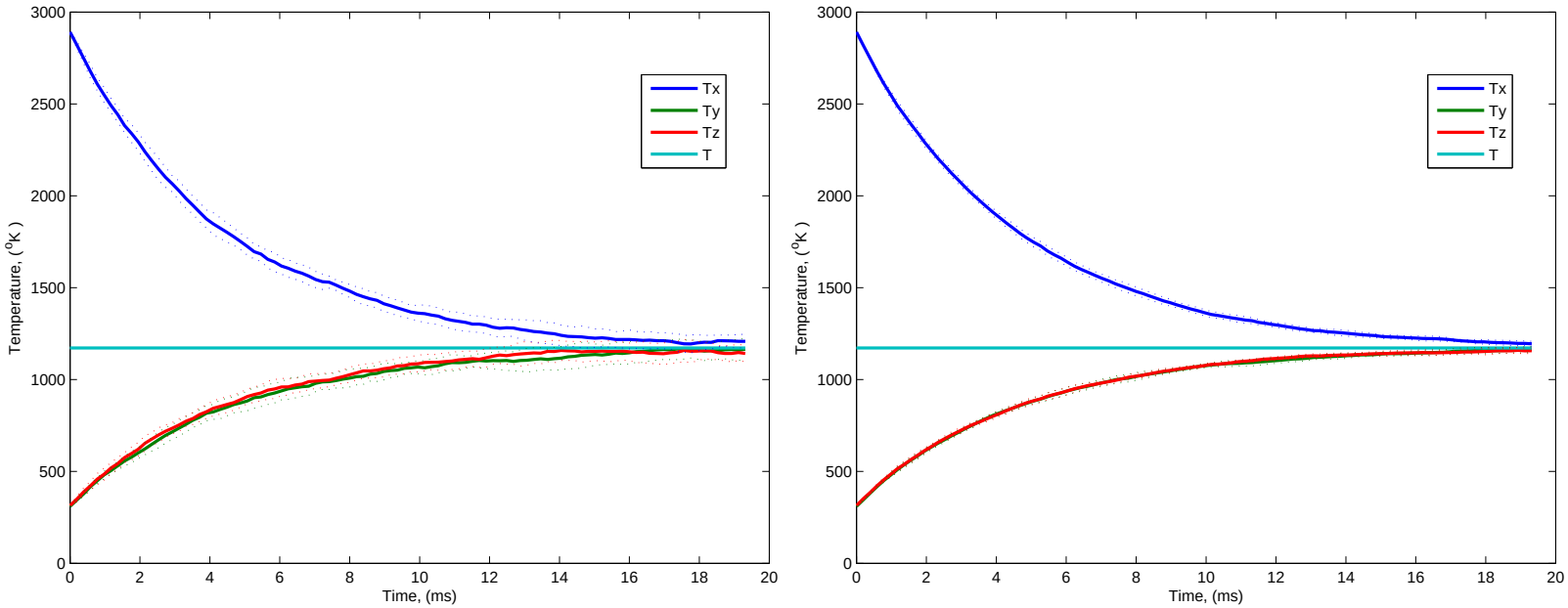

Mean and RMS Error of Sample Runs

Bi-Maxwellian Thermalization Results

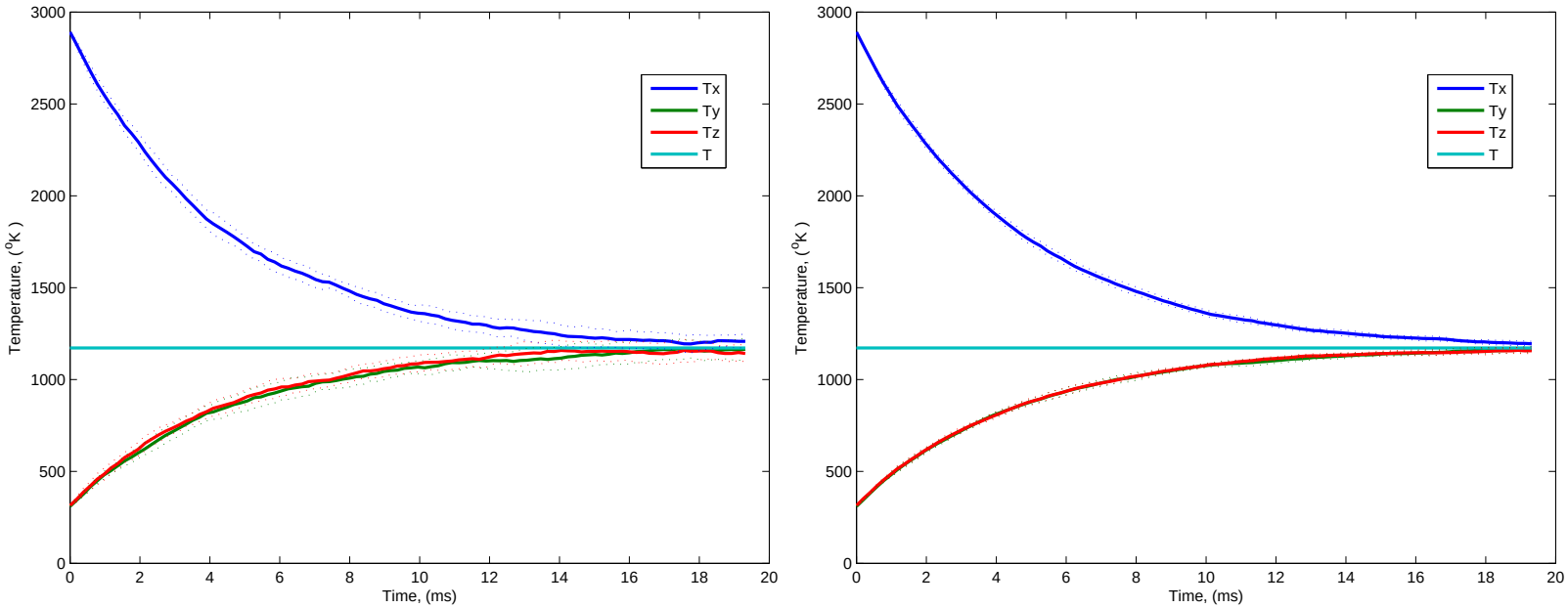

Mean and RMS Error of Sample Runs

Error Like Run with Many More Particles

Fractional Collision Selecting $n_c = f\, n_p\, log\, n_p$ Pairs

(Where f is a Free Parameter)

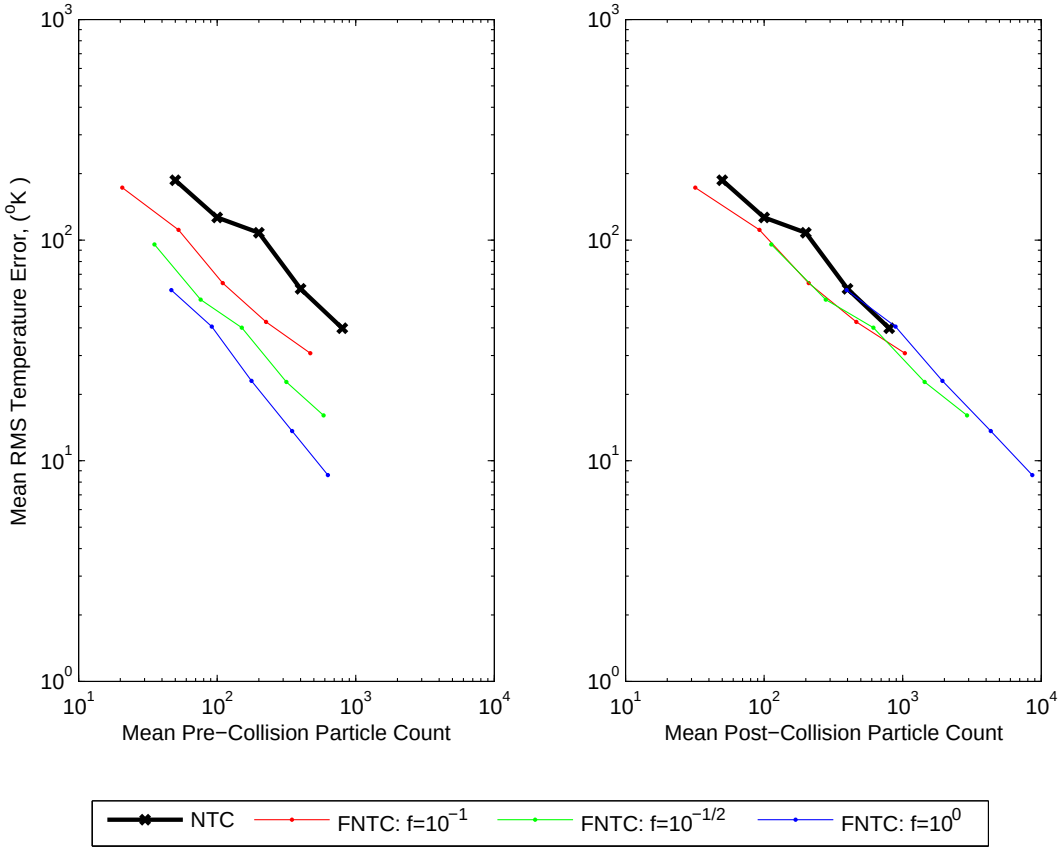

Higher f $\rightarrow$ Lower RMS Error

Coordinate $\rightarrow$ Post-Collision Count

Fractional Collision Selecting $n_c = f\, n_p\, log\, n_p$ Pairs

(Where f is a Free Parameter)

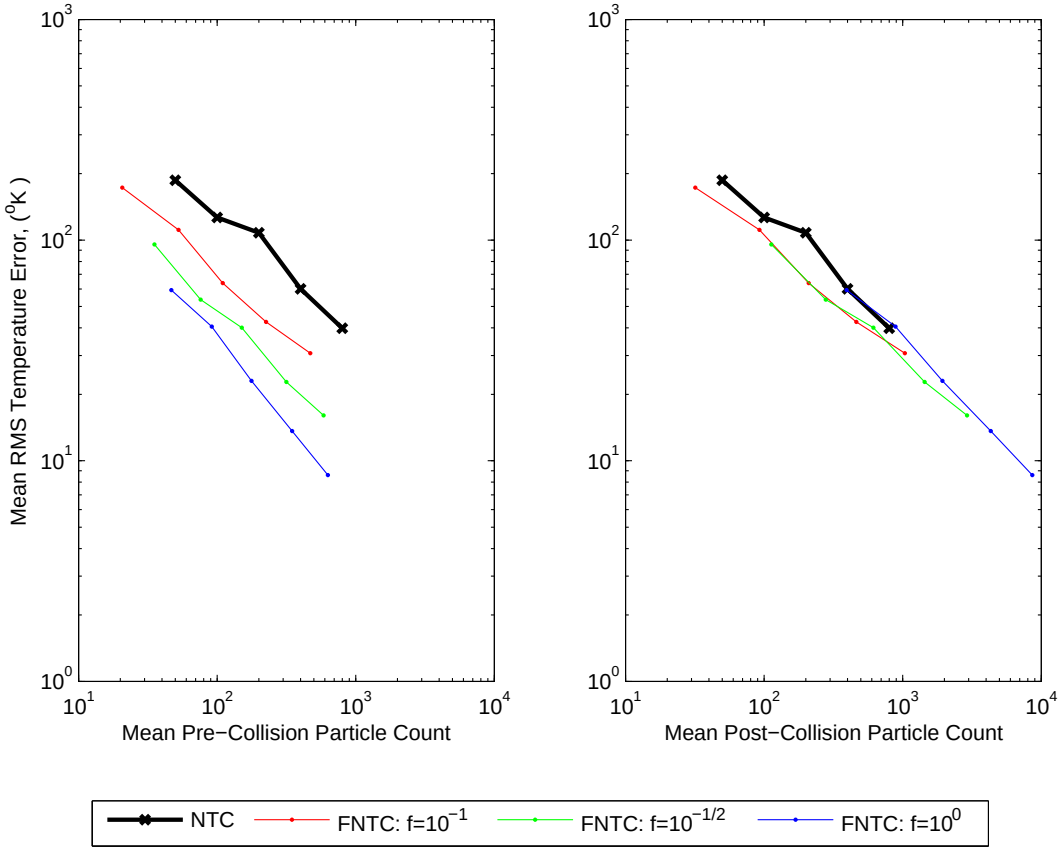

Higher f $\rightarrow$ Lower RMS Error Coordinate $\rightarrow$ Post-Collision Count

Error is Function of Post- not Pre-Collision Particle Count

Collisional Beams in Potential Well

- Initial Bi-Maxwellian Distribution in Potential Well

Collisional Beams in Potential Well

- Initial Bi-Maxwellian Distribution in Potential Well
- NTC Collisions Results in Beam Thermalization

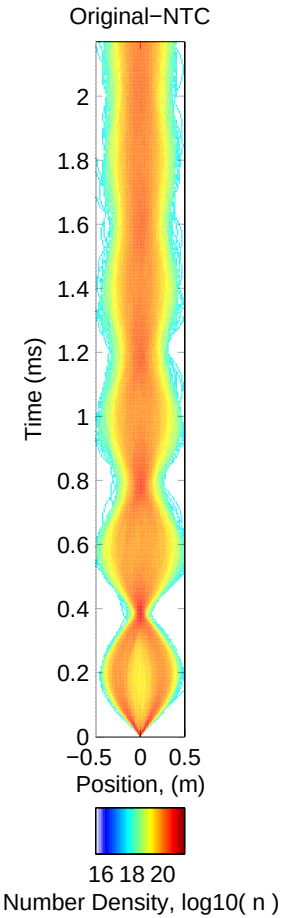

Collisional Beams in Potential Well

- Initial Bi-Maxwellian Distribution in Potential Well
- NTC Collisions Results in Beam Thermalization
- Fractional-NTC Collisions Produce Same Behavior

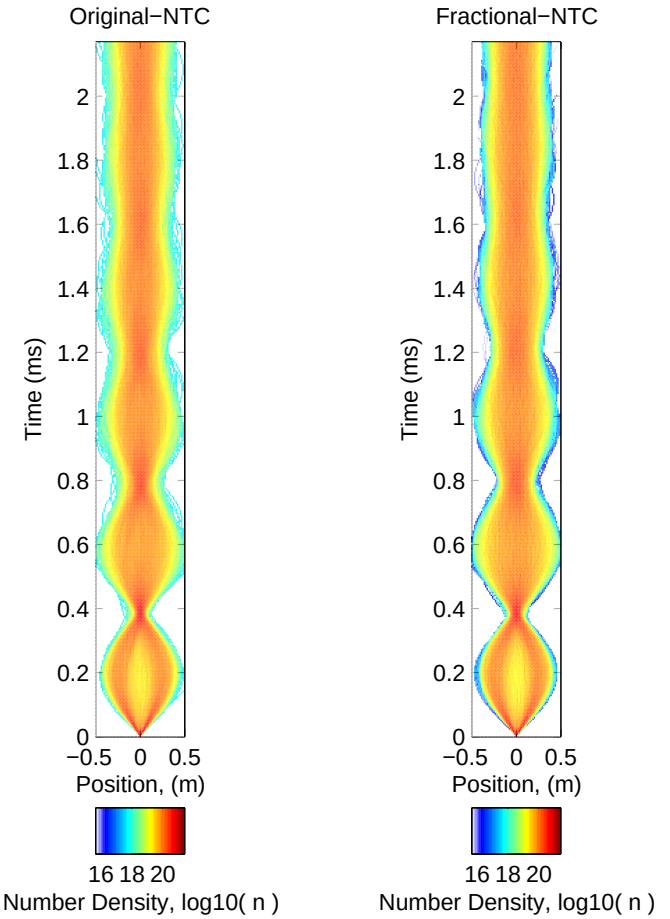

Collisional Beams in Potential Well

- Initial Bi-Maxwellian Distribution in Potential Well
- NTC Collisions Results in Beam Thermalization
- Fractional-NTC Collisions Produce Same Behavior
- Particles/Cell Dramatically Different

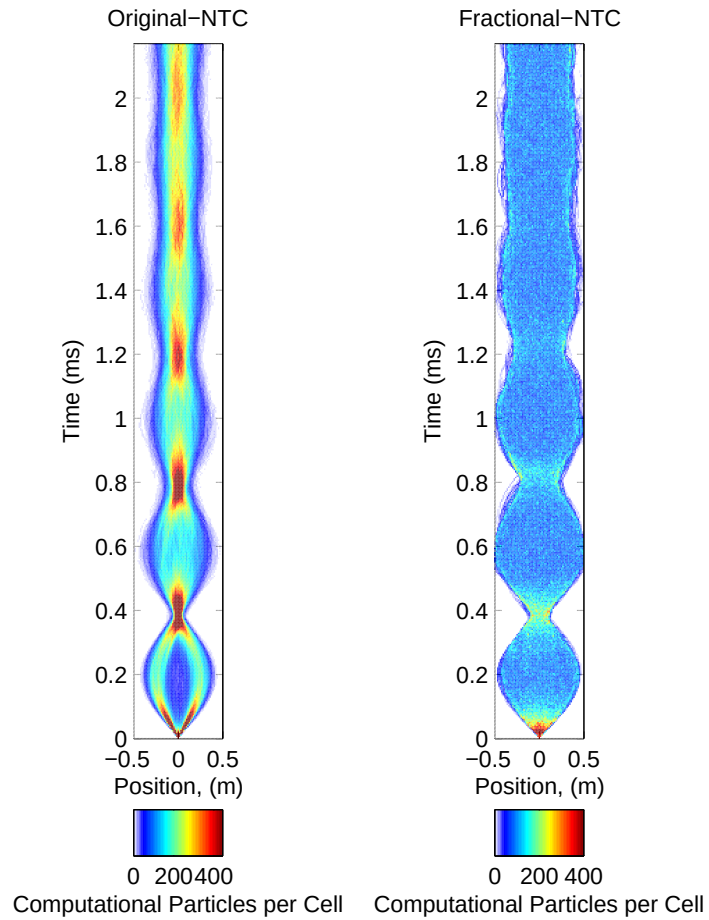

Collisional Beams in Potential Well

- Initial Bi-Maxwellian Distribution in Potential Well
- NTC Collisions Results in Beam Thermalization
- Fractional-NTC Collisions Produce Same Behavior
- Particles/Cell Dramatically Different
- Fringe Extends to Lower Densities with Variable Weights

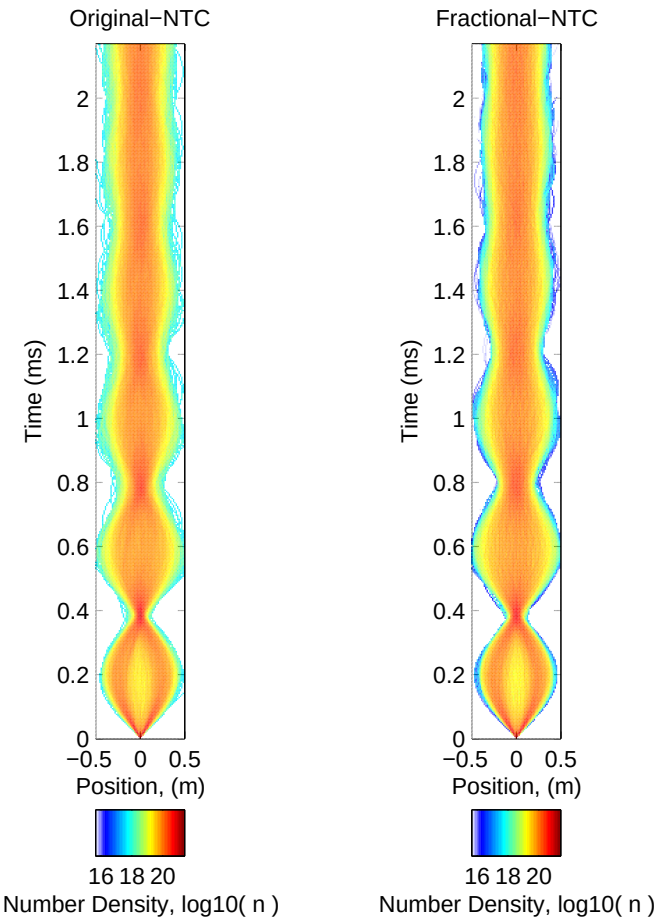

Collisional Beams in Potential Well

- Initial Bi-Maxwellian Distribution in Potential Well
- NTC Collisions Results in Beam Thermalization
- Fractional-NTC Collisions Produce Same Behavior
- Particles/Cell Dramatically Different
- Fringe Extends to Lower Densities with Variable Weights
- Relative 'Error' Unknown without Analytical Solution or High Fidelity Simulation

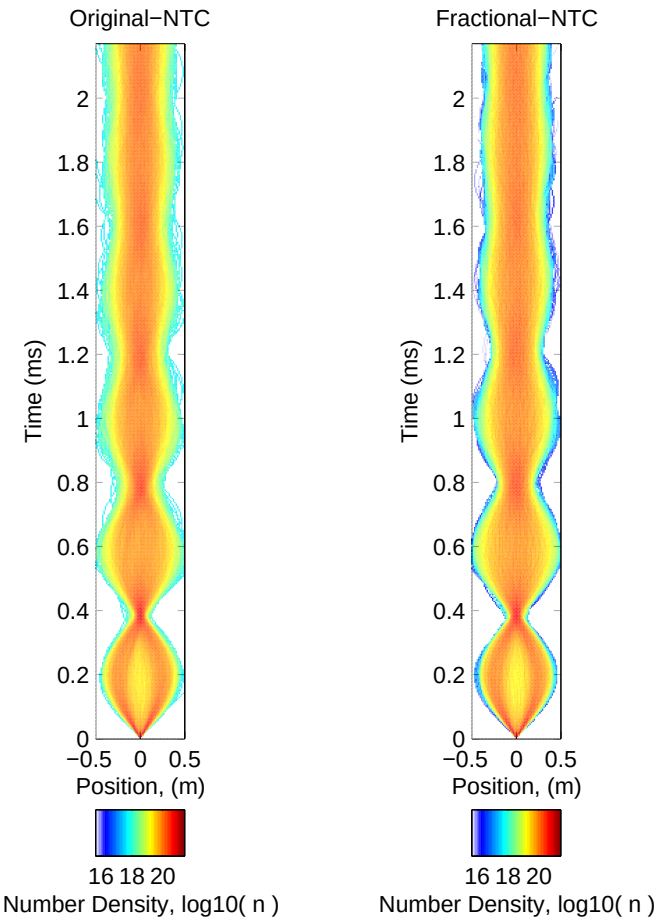

Fractional-MCC Gas Breakdown

- Ionizing Breakdown in 6kV Potential

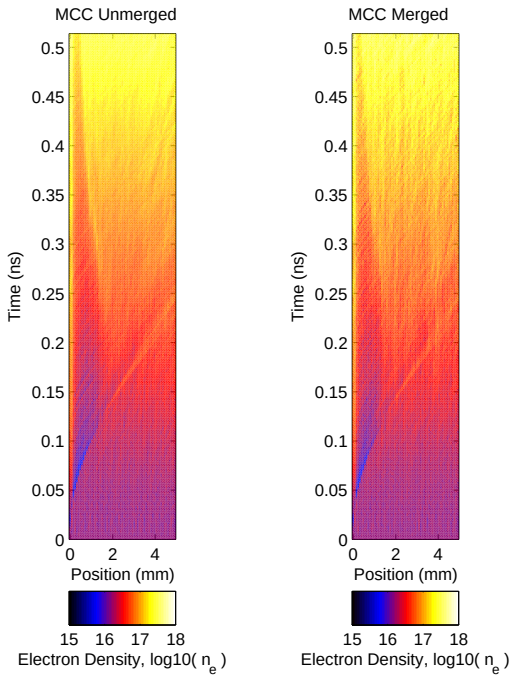

Fractional-MCC Gas Breakdown

- Ionizing Breakdown in 6kV Potential
- Electron Flow: Cathode $\rightarrow$ Anode

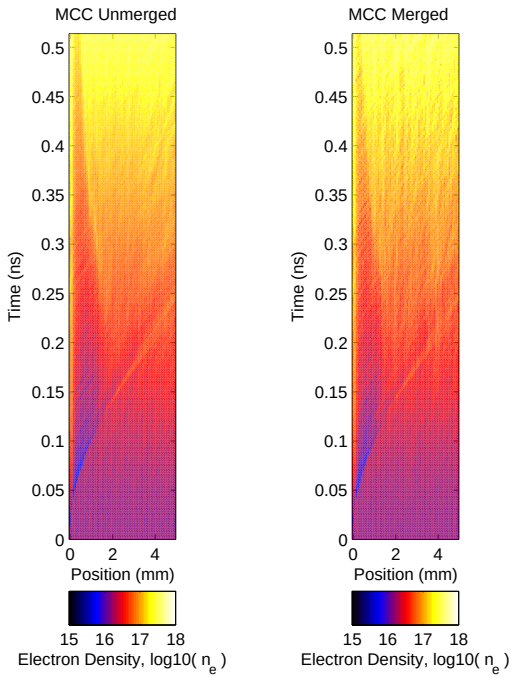

Fractional-MCC Gas Breakdown

- Ionizing Breakdown in 6kV Potential
- Electron Flow: Cathode $\rightarrow$ Anode
- Inelastic Fractional-MCC Version

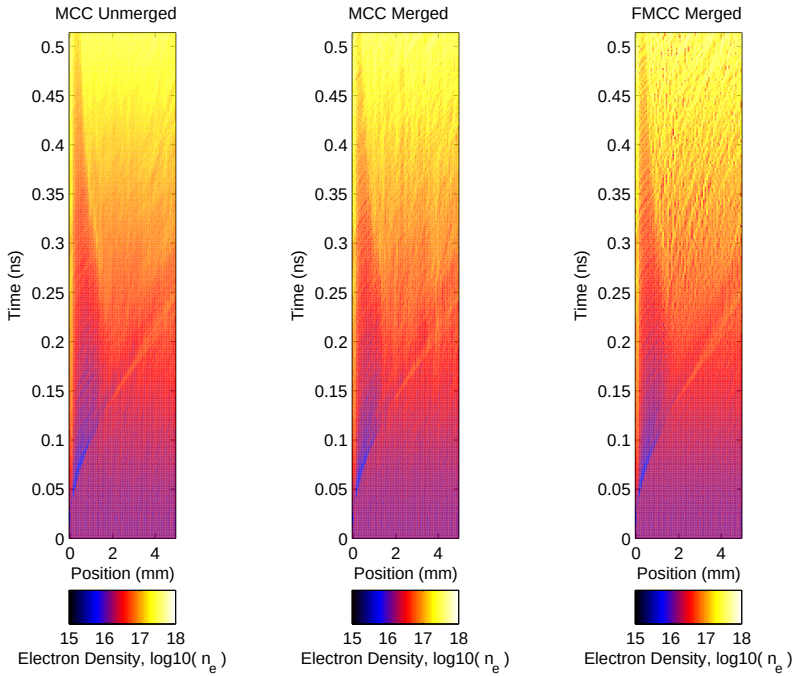

$$Ar^0 + e^- \rightarrow Ar^+ + (1-\alpha)e^-_{original} + \alpha e^-_{scattered} + \alpha e^-_{emitted}$$

Fractional-MCC Gas Breakdown

- Ionizing Breakdown in 6kV Potential
- Electron Flow: Cathode $\rightarrow$ Anode
- Inelastic Fractional-MCC Version
- Less Streaks Early

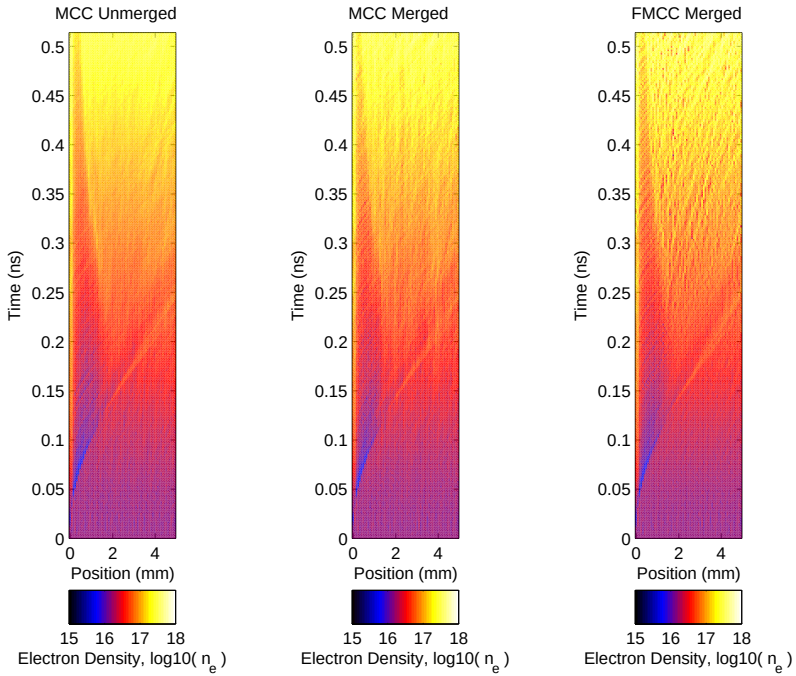

$$Ar^0 + e^- \rightarrow Ar^+ + (1-\alpha)e^-_{original} + \alpha e^-_{scattered} + \alpha e^-_{emitted}$$

Fractional-MCC Gas Breakdown

- Ionizing Breakdown in 6kV Potential
- Electron Flow: Cathode $\rightarrow$ Anode
- Inelastic Fractional-MCC Version
- Less Streaks Early
- More Noise Later

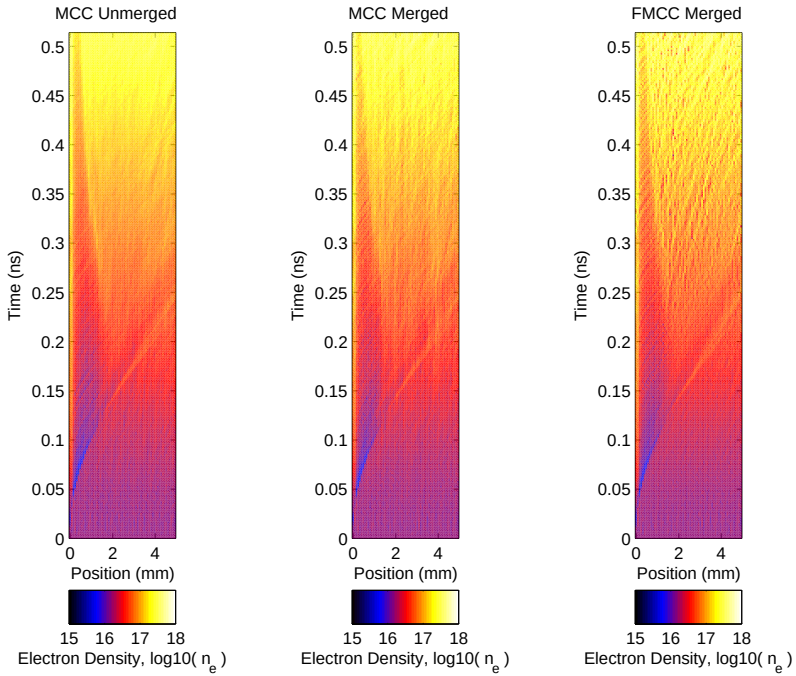

$$Ar^0 + e^- \rightarrow Ar^+ + (1-\alpha)e^-_{original} + \alpha e^-_{scattered} + \alpha e^-_{emitted}$$

Pseudo-Coulomb Collisions

Difficulty with Coulomb Collisions:

- Cross Section Diverges
- Cannot be Fully Represented Without N-body Interactions

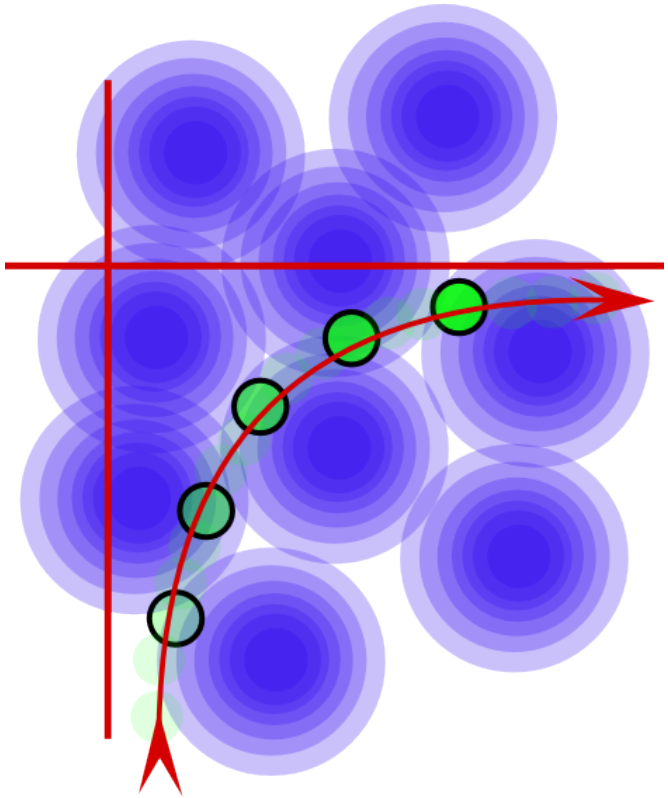

Pseudo-Coulomb Collisions

Difficulty with Coulomb Collisions:

- Cross Section Diverges
- Cannot be Fully Represented Without N-body Interactions
- Surrogate needed for Coulomb Thermalization

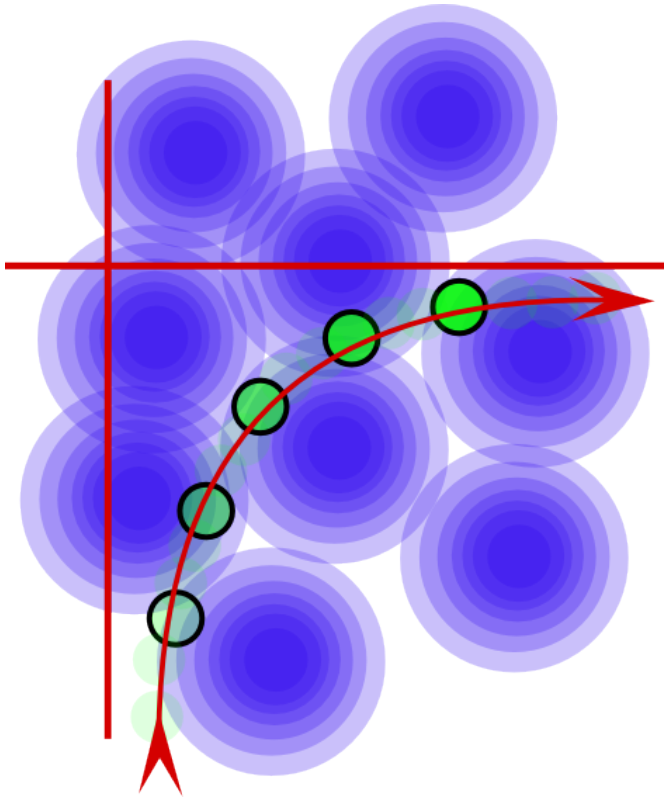

Pseudo-Coulomb Collisions

Difficulty with Coulomb Collisions:

- Cross Section Diverges
- Cannot be Fully Represented Without N-body Interactions
- Surrogate needed for Coulomb Thermalization
- Zel'dovich describes Combined Collisions $\approx$ to Original Momentum

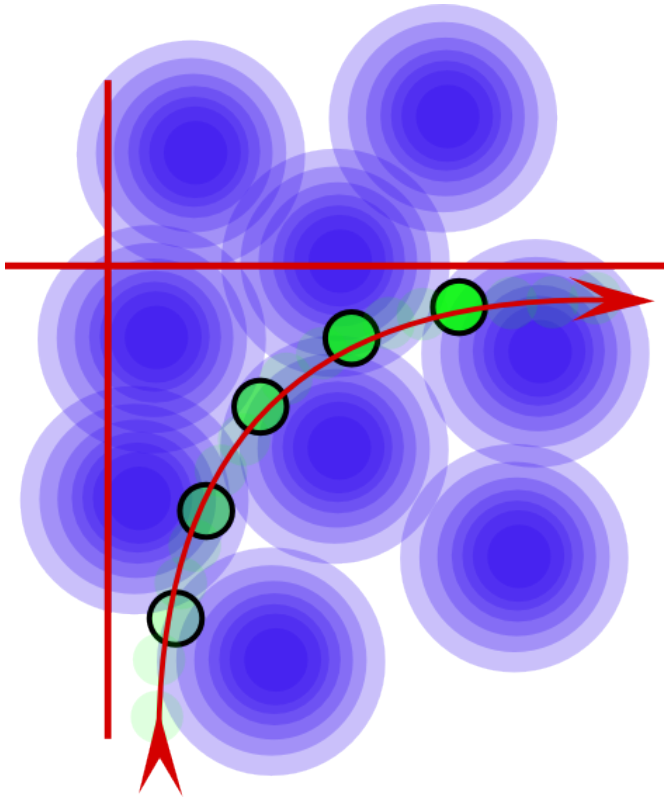

$$\sigma \approx \frac{4}{9}\pi \frac{Z^4 e^4}{kT^4}$$

Pseudo-Coulomb Collisions

Difficulty with Coulomb Collisions:

- Cross Section Diverges
- Cannot be Fully Represented Without N-body Interactions
- Surrogate needed for Coulomb Thermalization
- Zel'dovich describes Combined Collisions $\approx$ to Original Momentum
- Non-Equilibrium Cross Section to Reproduce Rate Attempted
- Early Results ΔT/Merge Dependent

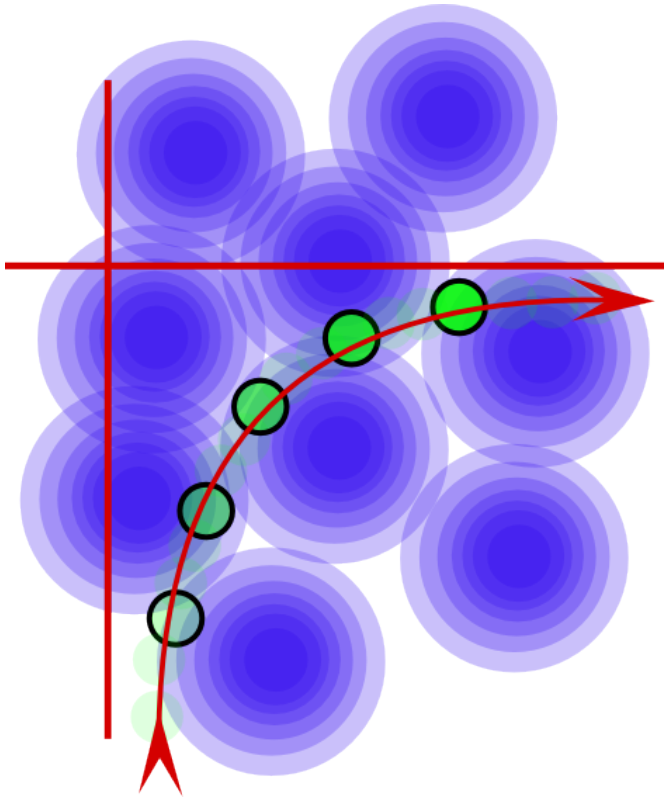

$$\sigma \approx \frac{4}{9}\pi \frac{Z^4 e^4}{kT^4}$$

Pseudo-Coulomb Collisions

Difficulty with Coulomb Collisions:

- Cross Section Diverges
- Cannot be Fully Represented Without N-body Interactions
- Surrogate needed for Coulomb Thermalization
- Zel'dovich describes Combined Collisions $\approx$ to Original Momentum
- Non-Equilibrium Cross Section to Reproduce Rate Attempted
- Early Results ΔT/Merge Dependent
- Cross-Section $\propto T^{-2} \approx v^{-4}$
  Must Conserve Higher Order Moments?

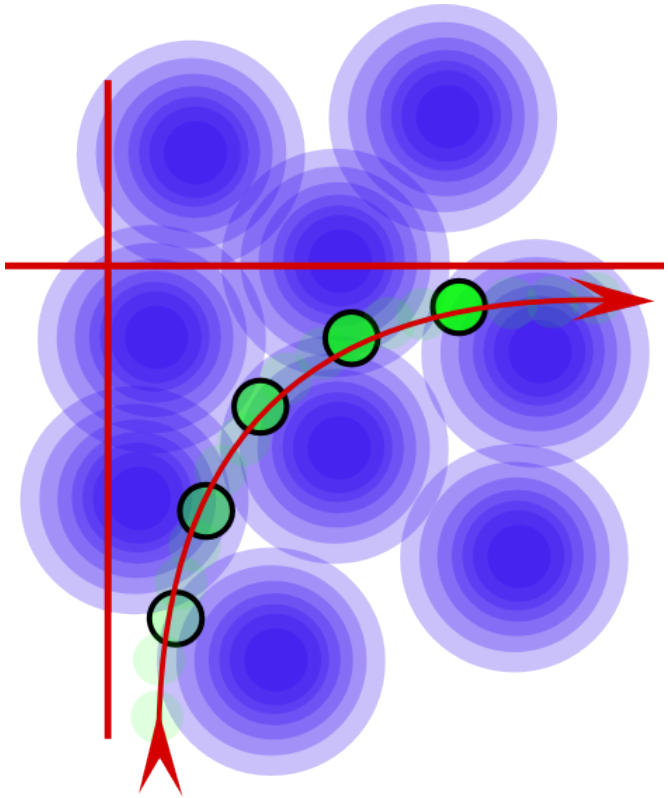

$$\sigma \approx \frac{4}{9}\pi \frac{Z^4 e^4}{kT^4}$$

Collision-Radiative Shock Ionization

Extending Applicability from 2-Fluid:

- Cellular Structures and Electron Avalanche Phenomena found in Shock-Ionization of Argon
- 2-Fluid Model Ignores Rarefaction/Non-Equilibrium Behavior
- Particle Code would Enable Rarefied Studies
- Future Hybridization of 2-Fluid/Particle would Enable Engine $\rightarrow$ Plume modeling of Spacecraft Electric Propulsion

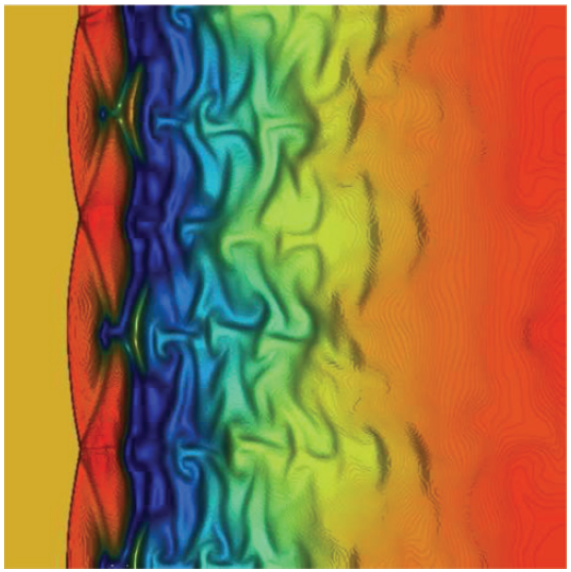

Kapper & Cambier, J. Appl. Phys. 109, (2011)

Thank You

Questions?